

# Optimal Participation of Heterogeneous, RES-based Virtual Power Plants in Energy Markets

Oluwaseun Oladimeji, Álvaro Ortega, Lukas Sigrist, Luis Rouco, Pedro Sánchez-Martín, Enrique Lobato  
Institute for Research in Technology, Comillas Pontifical University, Madrid, Spain

**Abstract**—In this work, we present a detailed model of an Renewable Energy Source (RES)-based Virtual Power Plant (VPP) that participates in Day-Ahead Market (DAM) and Intra-Day Market (IDM) with dispatchable and non-dispatchable RESs and flexible demand assets. We propose a demand model with bi-level flexibility which are associated with the market sessions plus an improved solar thermal plant model with piece-wise linear formulation of efficiency. A network-constrained unit commitment model is used by the VPP to submit DAM auctions and consequently participates in IDM to correct for deviations. Finally, we validate our model by assessing its operation on different weather conditions of uncertainty.

**Index Terms**—Day Ahead Market, Flexible Load, Intra-Day Market, Renewable Energy Sources, Solar Thermal Plants, Virtual Power Plant

## NOMENCLATURE

### Indexes and Sets

$b \in \mathcal{B}/\mathcal{B}^m$	Network Buses / Network buses Connected to Main Grid
$c \in \mathcal{C}/\mathcal{C}_b$	Dispatchable Renewable Energy Source (D-RES) / D-RES connected to bus $b$
$d \in \mathcal{D}/\mathcal{D}_b$	Demand / Demand connected to bus $b$
$k \in \mathcal{K}$	IDM sessions
$\ell \in \mathcal{L}$	Network lines
$p \in \mathcal{P}$	Demand profiles
$r \in \mathcal{R}/\mathcal{R}_b$	Non-dispatchable Renewable Energy Source (ND-RES) / ND-RES connected to bus $b$
$t \in \mathcal{T}$	Time periods
$\theta \in \Theta/\Theta_b$	Solar Thermal Unit (STU) / STU connected to bus $b$

### Parameters

$C_c^0/C_c^1$	Shut-down/start-up cost of D-RESs	[€]
$C_c^V$	Variable production cost of D-RESs	[€/MWh]
$C_{d,p}$	Cost of load profile $p$ of demand	[€]
$E_d$	Min energy consumption of demand $d$ throughout the planning horizon	[MWh]
$K_\theta$	STU $\theta$ output multiplier at startup	[–]
$\underline{P}_\theta/\bar{P}_\theta$	Min/max production capacity of STU $\theta$	[MW]
$\underline{P}_\theta^-/\bar{P}_\theta^-$	Lower/upper bound of discharging capacity of STU storage $\theta$	[MW]
$\underline{P}_c/\bar{P}_c$	Min/Max power production of D-RESs	[MW]
$\underline{P}_\theta^+/\bar{P}_\theta^+$	Lower/upper bound of charging capacity of STU storage $\theta$	[MW]
$\underline{P}_{d,t}/\bar{P}_{d,t}$	Lower/upper bound of the power consumption of demand $d$ in time $t$	[%]
$\underline{P}_{r,t}$	Min production of ND-RES in time $t$	[MW]
$\underline{P}_{d,p,t}$	Max hourly consumption of profile $p$ of demand $d$	[MW]
$\check{P}_{\theta,t}$	Available power production of STU in time $t$	[MW]
$\check{P}_{r,t}$	Available production of ND-RES in time $t$	[MW]

$\bar{P}_b^m$	Maximum power that can be traded with the main grid at bus $b$	[MW]
$\underline{R}_d/\bar{R}_d$	Down/up ramping limit of demand $d$	[MW/h]
$T$	Last period of schedule	[–]
$\Delta t$	Duration of time periods	[h, min]
$\eta_\theta^+/\eta_\theta^-$	Charging/discharging efficiency of STU storage	[%]
$\eta_\theta^0$	Conversion factor between thermal and electrical power in the PB of STU $\theta$ in segment $n \in \{1, 2, 3, 4\}$	[%]
$\lambda_t^{\text{DA}}$	DAM price in time $t$	[€/MWh]
$\lambda_{k,t}^{\text{ID}}$	Price of IDM session $k$ in time $t$	[€/MWh]

### Variables

$p_t^{\text{DA}}$	Total power traded in the DAM in time $t$	[MW]
$p_t^{\text{ID}}$	Total power traded in the IDM in time $t$	[MW]
$p_{\ell,t}$	Power flow through network of line $\ell$ in time $t$	[MW]
$p_{\theta,t}$	Electrical power generation of STU in time $t$	[MW]
$p_{\theta,t}^+/p_{\theta,t}^-$	Charging/discharging thermal power level of STU storage $\theta$ in time $t$	[MW <sub>t</sub> ]
$p_{\theta,t}^{\text{PB}}$	Thermal power delivered to the STU power block	[MW]
$p_{\theta,t}^{\text{SF}}$	Thermal power generated by the solar field	[MW]
$p_{b,t}^m$	Power scheduled to be bought from/sold to the DAM and IDM markets at bus $b$ in time $t$	[MW]
$p_{c,t}$	Power generation of D-RESs in time $t$	[MW]
$p_{d,t}$	Power consumption of demand in time $t$	[MW]
$p_{r,t}$	Power generation of ND-RES in time $t$	[MW]
$u_{\theta,t}$	Binary variable to control STU PB operation	[0/1]
$u_{\theta,t}^+$	Binary variable to control STU storage charging	[0/1]
$u_{d,p}$	Binary variable to select demand profile	[0/1]
$v_{\theta,t}^1$	Binary variable to control startup of STU PB $\theta$	[0/1]

## I. INTRODUCTION

Nowadays, RESs have emerged as a crucial part of modern power systems due mainly to their decreasing costs of operation and minimal carbon footprint. However, most RES technologies depend on sources of stochastic nature, and are non-dispatchable. Stochastic RESs thus have inherent disadvantage when participating in energy markets, as they are susceptible to economic penalties and/or losses if they do not supply the energy scheduled in the corresponding market session [1]. Additionally, they have relatively small sizes as single offering units compared with large conventional, synchronous plants.

The aggregation of RESs as VPPs to provide a more controllable output is a promising solution to improve the competitiveness of stochastic RESs in energy markets. A VPP participating in electricity markets and comprising only wind and solar PV power plants was presented in [2]. The uncertainties related to wind and irradiation were dealt with using appropriate forecasts and integrating the VPP operation with the distribution network. In [3], a VPP consisting of only stochastic RESs was analysed and energy storage systems

were utilized in providing the flexibility required to reduce the impact of generation uncertainty.

While models of the most common stochastic RES technologies such as wind and solar PV generation participating in energy markets are well established, appropriate modeling of other emerging technologies, e.g., Concentrated Solar Plant (CSP) is still an open issue. For instance, two aspects need to be carefully considered when modelling CSPs. These are integration of molten-salt thermal storage with the CSPs, and non-linear conversion efficiencies from thermal to electrical energy. The latter depend on the level of thermal power injected into the power block of the plant. CSPs with storage were modelled in [4] and [5] but conversion efficiency was chosen as an average value in both studies. Choosing a single average efficiency value might appear as a good compromise [6], but it does not correspond to actual operation of the CSP.

VPPs are also gradually including demands with flexibility provision capability in their portfolio [7]. However, a main challenge with demand side management models is the absence of appropriate structures of incentives for consumers that provide such flexibility actions. Flexible and non-flexible loads with associated costs were presented in [8] but these incentive measures were not addressed. A price-based control for demand management was proposed in [9] while neglecting the parametrization of the comfort of end users. In [10], the behaviour of dispatchable loads on an aggregated scale was studied but the end-goal in that work was decreasing the power system operation costs as well as reducing the need for conventional power plants.

In this regard, the contribution of this paper is a detailed model of heterogeneous, RES-based VPPs participating in energy markets. We propose:

- 1) a demand model with bi-level flexibility associated with different energy market trading sessions. In contrast to other studies, the demand owner sets different profiles which the VPP manager can choose from in DAM and allows tolerances around the chosen profile at IDM;
- 2) a detailed CSP model with storage capability. The model includes a linear formulation for the operation of CSP that addresses conversion from thermal to electrical energy using a piece-wise linear efficiency function; and
- 3) a network-constrained unit commitment model used by the VPP to submit DAM auctions and then subsequently participates in IDM sessions to correct for deviations of its ND-RES forecasts.

In this study, it is considered that the VPP participates in the Spanish energy market because of its separation of DAM and IDM, and ease of entrance of RESs [11]. However, no subsidies from the system or market operator are considered.

## II. OVERVIEW OF SPANISH ENERGY MARKET STRUCTURE

The wholesale electricity spot market in Spain is organised by the market operator (OMIE) [12] and system operator (Red Eléctrica de España (REE)) [13]. Two broad markets, the DAM and IDM, govern the day-to-day running of electricity provision and consumption with some additional arrangements

associated with ensuring reliability and secure operation of the energy system [14].

After DAM clearance, IDMs are instantiated to make adjustments to DAM cleared bids and correct infeasible schedules. These modifications or corrections can be due to unplanned shutdown of dispatchable sources of generation, changes in ND-RES outputs, demand changes and/or line faults. IDM sessions are especially useful for balancing renewable generation bid deficits or surplus by giving market participants with RESs an avenue to update their availability when their submitted DAM bids are different from near real time realizations. There are seven IDM sessions; the first and second cover 24 hours of the operation day while the remaining five sessions cover a receding subset of the 24 hours [14].

A consortium of generation and demand assets (a VPP), participating in the Spanish energy market can thus capture the operational flexibility which the different energy market segments offer in order to maximize its revenue. Our work, while currently tailored to the Spanish market, can be applied in other markets of similar characteristics and proves the potential of RES-based VPPs.

## III. VPP MODELLING

This section formulates and discusses the VPP model proposed in this paper. The VPP comprises Dispatchable Renewable Energy Sources (D-RESs) (hydro and biomass), Non-dispatchable Renewable Energy Sources (ND-RESs) (wind power plant, solar PV and solar thermal generation with storage capability) and flexible demands. These assets are distributed across the power network at different buses and connected to the main grid through one or more Points of Common Coupling (PCC). The business model considered for the VPP is maximization of its aggregated profit by optimally scheduling its generation and demand assets.

The formulation for each asset class is enumerated below. D-RES are modeled like conventional power plants [15] with linearized operation costs of the dispatchable assets. Network constraints are formulated using DC power flow [16]. The objective function of the VPP, and constraints for the ND-RESs, flexible demand, STU and energy balance at the PCCs are presented in the following subsections.

### A. Profit Maximization Objective

Due to small volumes of energy traded in the IDM relative to DAM and modest price differences between these markets [14], the objective functions in DAM and IDM are decoupled in this work. Each IDM further has associated constraints to cater for updates or changes in forecasts of stochastic sources. In DAM, the objective function (1) is the maximization of the obtainable profit by the VPP assets calculated as the revenue from power trades minus cost of operating D-RES and cost of selecting a particular load profile. For the different IDM sessions, the benefit (2) is calculated over changes in traded power  $\Delta p_{k,c,t}$  between: (i) DAM and first IDM trading period and (ii) other subsequent IDM sessions. Cost of choosing a specific load profile is not included while computing objective

of IDM because this choice is previously made during DAM participation and must be accounted for only once.

$$\max_{\Xi^{\text{DAM}}} \sum_{t \in \mathcal{T}} \left[ \lambda_t^{\text{DA}} p_t^{\text{DA}} \Delta t - \sum_{c \in \mathcal{C}} (C_c^{\text{V}} p_{c,t} \Delta t + c_{c,t}^0 + c_{c,t}^1) \right] - \sum_{d \in \mathcal{D}} \sum_{p \in \mathcal{P}} C_{d,p} u_{d,p} \quad (1)$$

$$\max_{\Xi_k^{\text{IDM}}} \sum_{t=\tau_k}^{|\mathcal{J}|} \left[ \lambda_{k,t}^{\text{ID}} p_{k,t}^{\text{ID}} \Delta t - \sum_{c \in \mathcal{C}} (C_c^{\text{V}} \Delta p_{k,c,t} \Delta t + c_{k,c,t}^0 + c_{k,c,t}^1) \right], \quad \forall k \in \mathcal{K} \quad (2)$$

## B. Energy Balance

Energy balance constraints common to both market stages are modeled in (3) whereas those specific to DAM and IDM are formulated in (4) and (5) respectively. Nodal analysis is utilized, implying that at each bus of the network, sum of inflows and outflows must be equal. Equation (3a) gives energy balance at the Point of Common Coupling (PCC) with the main grid while (3b) is the balance for all other buses in the VPP network at every time period [17]. The difference between both equations is the presence of  $p_{b,t}^m$  at the main grid representing scheduled power to be traded with other market participants. This power available for trading (buy or sell) is set within prespecified bounds in (3c).

$$\sum_{c \in \mathcal{C}_b} p_{c,t} + \sum_{r \in \mathcal{R}_b} p_{r,t} + \sum_{\theta \in \Theta_b} p_{\theta,t} - \sum_{\ell | i(\ell)=b} p_{\ell,t} + \sum_{\ell | j(\ell)=b} p_{\ell,t} = p_{b,t}^m + \sum_{d \in \mathcal{D}_b} p_{d,t}, \quad \forall b \in \mathcal{B}^m, \forall t \in \mathcal{T} \quad (3a)$$

$$\sum_{c \in \mathcal{C}_b} p_{c,t} + \sum_{r \in \mathcal{R}_b} p_{r,t} + \sum_{\theta \in \Theta_b} p_{\theta,t} - \sum_{\ell | i(\ell)=b} p_{\ell,t} + \sum_{\ell | j(\ell)=b} p_{\ell,t} = \sum_{d \in \mathcal{D}_b} p_{d,t}, \quad \forall b \in \mathcal{B} \setminus \mathcal{B}^m, \forall t \in \mathcal{T} \quad (3b)$$

$$-\bar{P}_b^m \leq p_{b,t}^m \leq \bar{P}_b^m, \quad \forall b \in \mathcal{B}^m, \forall t \in \mathcal{T} \quad (3c)$$

1) *DAM Formulation:* Equation (4a) ensures that summation of traded power at all buses connected to the main grid is equivalent to the total power available for trading by VPP whereas (4b) relaxes this available power at each time period.

$$p_t^{\text{DA}} = \sum_{b \in \mathcal{B}^m} p_{b,t}^m, \quad \forall t \in \mathcal{T} \quad (4a)$$

$$-\left( \sum_{d \in \mathcal{D}} P_{d,p,t} + \sum_{\theta \in \Theta} \bar{P}_{\theta}^+ \right) \leq p_t^{\text{DA}} \leq \sum_{c \in \mathcal{C}} \bar{P}_c + \sum_{r \in \mathcal{R}} \check{P}_{r,t} + \sum_{\theta \in \Theta} \bar{P}_{\theta}, \quad \forall p \in \mathcal{P}, \forall t \in \mathcal{T} \quad (4b)$$

2) *IDM Formulation:* For IDM sessions, the bounds on the traded power are modified such that the load profile that was chosen in the DAM is taken into account as formulated in (5a). Note that the IDM offers/bids do not substitute those submitted in the DAM, but rather, they are *adjustments* of

the DAM offers/bids as reflected in (5b). The rationale behind such adjustments is duly justified in Sections II and III-C.

$$-\left( \sum_{d \in \mathcal{D}} (1 + \bar{P}_{d,t}) P_{d,p,t}^{\text{P}^*} + \sum_{\theta \in \Theta} \bar{P}_{\theta}^+ \right) \leq p_t^{\text{DA}^*} + \sum_{\kappa=1}^{k-1} p_{\kappa,t}^{\text{ID}^*} + p_{k,t}^{\text{ID}} \leq \sum_{c \in \mathcal{C}} \bar{P}_c + \sum_{r \in \mathcal{R}} \check{P}_{r,t} + \sum_{\theta \in \Theta} \bar{P}_{\theta}, \quad \forall k \in \mathcal{K}, \forall t \geq \tau \quad (5a)$$

$$p_t^{\text{DA}^*} + \sum_{\kappa=1}^{k-1} p_{\kappa,t}^{\text{ID}^*} + p_{k,t}^{\text{ID}} = \sum_{b \in \mathcal{B}^m} p_{b,t}^m, \quad \forall k \in \mathcal{K}, \forall t \geq \tau \quad (5b)$$

In (5),  $p_t^{\text{DA}^*}$  and  $p_t^{\text{ID}^*}$  are the solutions of the DAM and previous IDMs respectively; and  $P_{d,p,t}^{\text{P}^*}$  is the optimal load profile for each demand, scaled by the profile's upper bound of uncertainty,  $\bar{P}_{d,t}$ , (see (5a)). Note that for the nodal equations,  $\forall t \in \mathcal{T}$ , is replaced with  $\forall t \geq \tau$ , where  $\tau$  is the first delivery period of the current IDM session.

## C. Non-dispatchable Renewable Energy Sources

The ND-RESs modeled in (6) comprise mainly wind power and solar PV plants. The lower bound represents the asset technical minimum (e.g., cut-in speed for wind plant) while the output is bounded above by the available stochastic source.

$$P_{r,t} \leq p_{r,t} \leq \check{P}_{r,t}, \quad \forall r \in \mathcal{R}, \forall t \in \mathcal{T} \quad (6)$$

## D. Solar Thermal Units

STUs are synchronous generating plants that rely on a stochastic renewable source (solar irradiation). Additionally, they usually include storage capability for as much as 8 hours at full power capacity [18]. Moreover, conversion between thermal and electrical power that takes place in the Power Block (PB) of the STU needs to be appropriately formulated. For these reasons, STUs cannot be accurately represented by parametrizing any of the sets of constraints above, and they require a specific set in the VPP model proposed in this paper.

Equation (7a) defines upper and lower bounds of the active power (thermal) that can be generated by the solar field,  $p_{\theta,t}^{\text{SF}}$ , which is only limited by the available power extractable from solar irradiation. The charging and discharging power (thermal) of the STU storage device are bounded above and below in (7b) and (7c). The power (thermal),  $p_{\theta,t}^{\text{PB}}$ , sent to the PB which converts the thermal into electrical power through a synchronous turbine, is given in (7d). It is the sum of the thermal power generated by the solar field, net thermal power of the STU storage and a final factor containing coefficient  $K_{\theta}$  that takes startup losses into account. This power is then bounded in (7e) by the maximum and minimum power output of the turbine. The commitment status of the PB reflecting its on/off status is modeled like dispatchable power plants.

Electrical power output of the STU is given by (7f). Conversion between thermal and electrical power is nonlinear, and depends on the level of thermal power injected into the PB. The higher  $p_{\theta,t}^{\text{PB}}$  is, the more efficient the conversion. In this work, we have defined four linear segments, delimited by  $P_{\theta}^{\text{PB}} = \{\underline{P}_{\theta}^{\text{PB}}, P_{\theta}^{\text{PB},1}, P_{\theta}^{\text{PB},2}, \bar{P}_{\theta}^{\text{PB}}\}$ , and characterized by

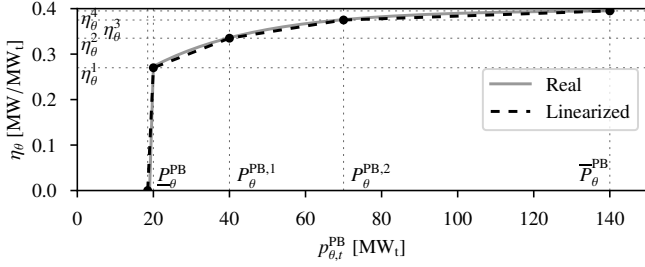


Fig. 1. Power Block conversion efficiency

different conversion factors,  $\eta_\theta = \{\eta_\theta^1, \eta_\theta^2, \eta_\theta^3, \eta_\theta^4\}$ . Fig. 1 shows the PB efficiency for converting thermal power input into electric power using parameters for a 50 MW STU in Spain.

Finally, equations that model the thermal energy stored in the STU storage device are (7g)-(7j) where  $\bar{E}_{\theta,t}$  is the thermal storage capacity and  $\underline{\alpha}_\theta/\bar{\alpha}_\theta$  is the lower/upper bound multiplier of storage at the final period of the schedule.

$$0 \leq p_{\theta,t}^{\text{SF}} \leq \check{P}_{\theta,t}, \quad \forall \theta \in \Theta, \forall t \in \mathcal{T} \quad (7a)$$

$$P_{\theta,t}^+ u_{\theta,t}^+ \leq p_{\theta,t}^+ \leq \check{P}_{\theta,t} u_{\theta,t}^+, \quad \forall \theta \in \Theta, \forall t \in \mathcal{T} \quad (7b)$$

$$(1 - u_{\theta,t}^+) P_{\theta,t}^- \leq p_{\theta,t}^- \leq (1 - u_{\theta,t}^+) \check{P}_{\theta,t}^-, \quad \forall \theta \in \Theta, \forall t \in \mathcal{T} \quad (7c)$$

$$p_{\theta,t}^{\text{PB}} = p_{\theta,t}^{\text{SF}} + p_{\theta,t}^- - p_{\theta,t}^+ - K_\theta v_{\theta,t}^1 \bar{P}_{\theta,t}^{\text{PB}}, \quad \forall \theta \in \Theta, \forall t \in \mathcal{T} \quad (7d)$$

$$u_{\theta,t} P_{\theta,t}^{\text{PB}} \leq p_{\theta,t}^{\text{PB}} \leq u_{\theta,t} \bar{P}_{\theta,t}^{\text{PB}}, \quad \forall \theta \in \Theta, \forall t \in \mathcal{T} \quad (7e)$$

$$p_{\theta,t} = \begin{cases} \eta_\theta^1 p_{\theta,t}^{\text{PB}} & \text{if } 0 \leq p_{\theta,t}^{\text{PB}} < P_{\theta,t}^{\text{PB}} \\ \eta_\theta^2 p_{\theta,t}^{\text{PB}} & \text{if } P_{\theta,t}^{\text{PB}} \leq p_{\theta,t}^{\text{PB}} < P_{\theta,t}^{\text{PB},1} \\ \eta_\theta^3 p_{\theta,t}^{\text{PB}} & \text{if } P_{\theta,t}^{\text{PB},1} \leq p_{\theta,t}^{\text{PB}} < P_{\theta,t}^{\text{PB},2} \\ \eta_\theta^4 p_{\theta,t}^{\text{PB}} & \text{if } P_{\theta,t}^{\text{PB},2} \leq p_{\theta,t}^{\text{PB}} \leq \bar{P}_{\theta,t}^{\text{PB}} \end{cases}, \quad \forall \theta \in \Theta, \forall t \in \mathcal{T} \quad (7f)$$

$$e_{\theta,t} = e_{\theta,(t-1)} + p_{\theta,t}^+ \Delta t \eta_\theta^+ - \frac{p_{\theta,t}^- \Delta t}{\eta_\theta^-}, \quad \forall \theta \in \Theta, \forall t \in \mathcal{T} \quad (7g)$$

$$\bar{E}_{\theta,t} \leq e_{\theta,t} \leq \bar{E}_{\theta,t}, \quad \forall \theta \in \Theta, \forall t \in \mathcal{T} \quad (7h)$$

$$\underline{\alpha}_\theta \bar{E}_{\theta,t} \leq e_{\theta,t} \leq \bar{\alpha}_\theta \bar{E}_{\theta,t}, \quad \forall \theta \in \Theta, t = T \quad (7i)$$

$$0 \leq \underline{\alpha}_\theta \leq \bar{\alpha}_\theta \leq 1, \quad \forall \theta \in \Theta \quad (7j)$$

$$u_{\theta,t}, u_{\theta,t}^+, v_{\theta,t}^1 \in \{0, 1\}, \quad \forall \theta \in \Theta, \forall t \in \mathcal{T} \quad (7k)$$

Note that, for implementation purposes, the piece-wise linear function, (7f), is remodelled with SOS-2 constraints [19].

### E. Flexible Demands

In this work, we present a novel participation of flexible demands in a VPP comprising two levels of flexibility which are associated with the DAM and IDM market sessions.

1) *DAM Formulation*: At the first stage, such participation involves the selection of a specific load profile. With this aim, (8a) and (8b) ensure that for each demand  $d$ , only one load profile  $p$  out of all available profiles is selected. These profiles mirror the different available operational characteristics of the demand assets. e.g. for residential demand, a profile might feature dual peaks at 09:00 and 20:00 while another profile features a shift of the peaks to 07:00 and 21:00 respectively. These profiles are prepared by the demand owners/aggregators and subsequently communicated to the VPP manager. One of them could be the default profile which the load owner

will follow if no coordination exists. Other profiles which can offer flexibility but might lead to higher operation costs for the load owner can be presented and the VPP manager needs to compensate them in exchange for the offered flexibility if those profiles are selected.

$$p_{d,t} = \sum_{p \in \mathcal{P}} P_{d,p,t} u_{d,p}, \quad \forall d \in \mathcal{D}, \forall t \in \mathcal{T} \quad (8a)$$

$$\sum_{p \in \mathcal{P}} u_{d,p} = 1, \quad \forall d \in \mathcal{D} \quad (8b)$$

$$u_{d,p} \in \{0, 1\}, \quad \forall d \in \mathcal{D}, \forall p \in \mathcal{P} \quad (8c)$$

2) *IDM Formulation*: The second level of demand flexibility is provided during the different IDM sessions, formulated in (9). At IDM, the load profile selected from DAM cannot be changed. However, the demand owner allows the VPP manager to vary the consumption a small percentage above and below that selected profile ( $P_{d,p,t}^*$ ) as presented in (9a). These bounds on the demand may or may not be symmetric; and are chosen in this paper as a reflection of realistic practises. Equations (9b) and (9c) define the ramps of the demand profile from one period to the next. Finally, (9d) ensures that, over the total duration of the current IDM session plus the periods covered in previous sessions, a minimum amount of energy is consumed. The energy values settled in previous periods,  $p_{d,t}^*$ , are thus accounted for during subsequent IDM.

$$(1 - \underline{P}_{d,t}) P_{d,p,t}^* \leq p_{d,t} \leq (1 + \bar{P}_{d,t}) P_{d,p,t}^*, \quad \forall d \in \mathcal{D}, \forall t \geq \tau \quad (9a)$$

$$p_{d,t} - p_{d,(t-1)} \leq \bar{R}_d \Delta t, \quad \forall d \in \mathcal{D}, \forall t \geq \tau \quad (9b)$$

$$p_{d,(t-1)} - p_{d,t} \leq \underline{R}_d \Delta t, \quad \forall d \in \mathcal{D}, \forall t \geq \tau \quad (9c)$$

$$\underline{E}_d \leq \sum_{t=1}^{\tau-1} p_{d,t}^* \Delta t + \sum_{t=\tau}^{|\mathcal{T}|} p_{d,t} \Delta t, \quad \forall d \in \mathcal{D} \quad (9d)$$

## IV. CASE STUDY

This section presents the case studies considered to test and validate the RES-based VPP model proposed in this paper. Section IV.A outlines the VPP topology considered, which resembles a subarea of the southern region of the Spanish grid. The input data that is fed into the model is then described in Section IV.B. Finally, Section IV.C presents and discusses the simulation results. These case studies are implemented in GAMS with CPLEX on a computer with 32GB memory, intel i7 and run-time (reading of data, algorithm execution and writing of results) is less than 5 seconds for all scenarios.

### A. VPP Description

The VPP assets are distributed across a 12-node network connected to a main grid through a PCC as shown in Fig. 2. The capacities of D-RESs, hydro (bus 6) and biomass (bus 9) are 111 and 5 MW respectively. For ND-RESs, wind power plant (bus 4), solar PV (bus 8) and STU (bus 1) power block have rated capacities of 50 MW each. The thermal storage capacity associated with the STU is 1100 MWh<sub>th</sub>. It is desired that, after an operation day, a predefined amount of such capacity is reserved for first period of the next operation day

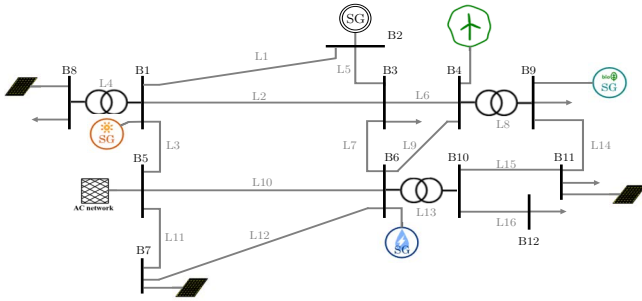


Fig. 2. 12-node network for test cases

such that it might be used to capture some benefits of early high prices before another charging period begins (see eqs. (7i) and (7j)). Additionally, thermal storage can only be charged from the solar field and not from the main grid. The demands considered are industrial, airport and residential loads (buses 3, 9 and 12) with minimum daily consumption of 800, 580, and 600 MWh respectively. Three profiles are associated with each demand and total consumption for each profile is same.

### B. Input Parameters

A time horizon of 24 hours with an hourly timescale is utilized during DAM, while a subset of the 24 hours is used for each IDM session (see [14]). The VPP has the possibility to supply its internal demand, partially or entirely, by buying energy from the main grid at the PCCs if needed. In our case, the maximum value of energy that the VPP can buy is 110 MWh. Furthermore, we make computations for different seasons and days based on historical data of actual and forecast profiles. Fig. 3 shows estimated wind power output and irradiation levels in Southern Spain for a clear, sunny day in March 2014 and a day with cloud covers in March 2018.

For demands, we show as example two of the three loads: airport (A) and residential (R) with three different profiles ('bc-basecase', 'ep-early peak', 'lp-late peak') in Fig. 4. While fictitious, the base profile replicates *default activities* of airport and residential electricity consumers while other profiles are designed to perform peak shifting around it. During IDM, the demand owner allows a 10% tolerance for demand movement over the selected profile at DAM.

In Fig 5, representative prices for DAM and all IDM sessions for both clear and cloudy days are presented.

### C. Results

To test the effectiveness of our model, we identify two operation strategies:

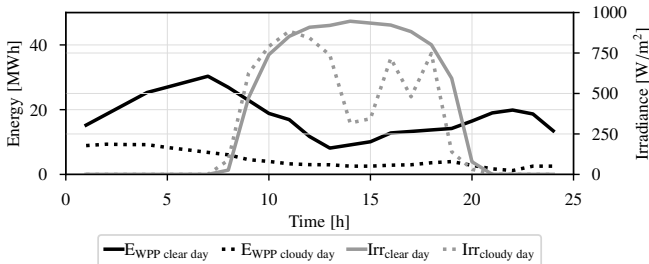


Fig. 3. Forecasts for STU, WPP & PV generation on a clear and cloudy day

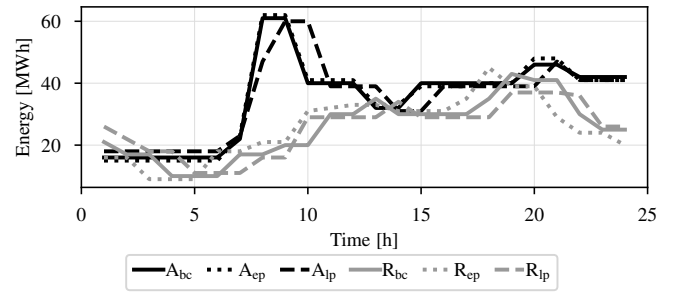


Fig. 4. Airport and residential demand profiles

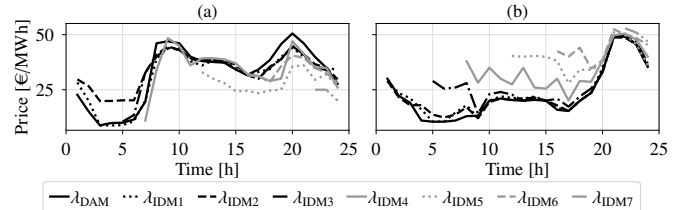


Fig. 5. DAM and IDM prices on (a) clear day, (b) cloudy day

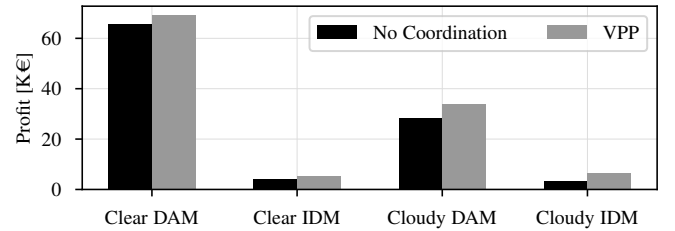


Fig. 6. VPP benefits on different strategies

- Base case where generation or consumption units act individually (No Coordination).
- Coordinated VPP operation as formulated in Section III.

First, we outline the benefits of the VPP strategic behaviour over the No Coordination case for the DAM and the first IDM session with a default load profile in both cases. Profit comparison between the days and the strategies is shown in Fig. 6. For the clear day, there is a 5% and 28% increase in the profits during DAM and IDM respectively when the VPP model is compared to the case without coordination. However, these profits are more significant during the cloudy day where the VPP outperforms the base case with 20% and 99% during DAM and IDM respectively.

To fully comprehend the effectiveness of the presented VPP model, we analyse the following scenarios in detail: firstly, a clear day with high wind power plant output, high irradiance level, and secondly, a day with intermittent cloud covers in the afternoon and low wind power output. Each of these two broad categorisations will be further examined under (a) Base case with default load profile (b) VPP with default load profile and (c) VPP with three load profiles at zero cost. Finally, we conduct an analysis to ascertain the behaviour of non-zero cost demand profiles on a clear day.

#### 1) Traded Power and Output of Assets on a Clear Day:

Fig. 7 shows traded power on a clear day during DAM and all IDM sessions and Fig. 8 depicts the expected behaviour of the different assets at DAM. The effect of coordination is evident

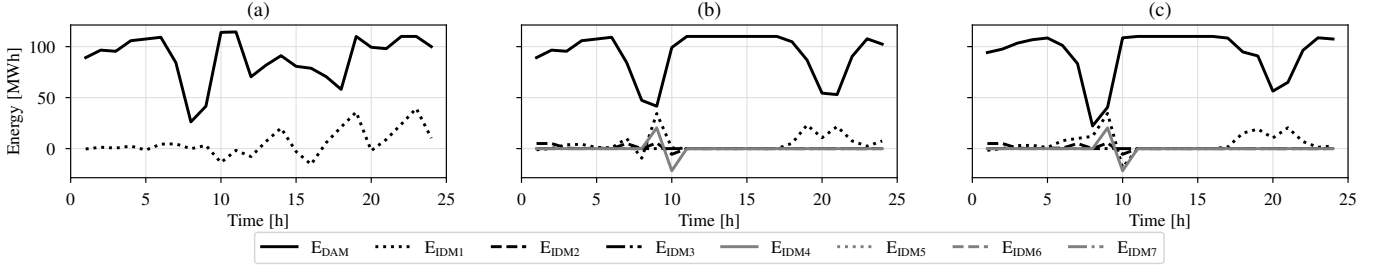


Fig. 7. Traded power on a clear day at DAM & IDM in: (a) No Coordination, (b) VPP with default load profile, (c) VPP with three load profiles at zero cost

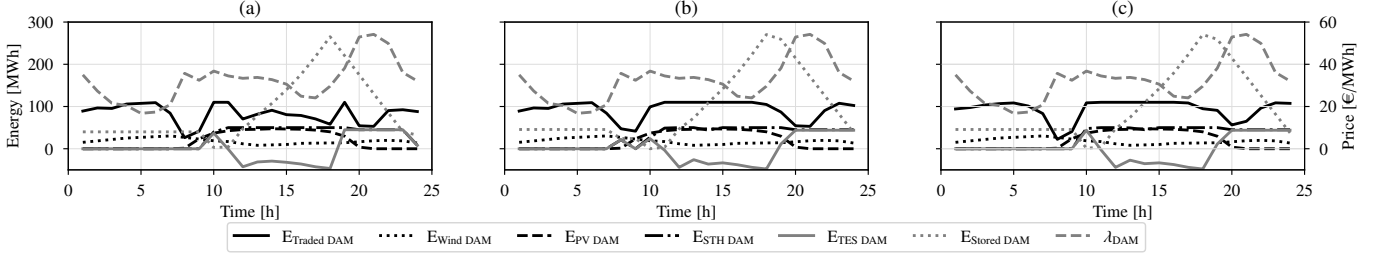


Fig. 8. Output of assets at DAM on a clear day: (a) No Coordination, (b) VPP with default load profile, (c) VPP with three load profiles at zero cost

from the smoothing of the traded power curve from period 10h-16h in VPP compared with the base case. The differences arise largely due to proper synchronization of the STU with its storage and the biomass plant response to the market price. The low volume of energy traded in period 8h-9h coincide with very high demand and relatively low generation in the three cases. Moreover, in terms of benefits to the VPP, case (c) with three load profiles at zero cost has the highest profit because it leverages differences in the load shape and chooses the best profile to suit its objective. The residential early peak profile was selected in this instance while the basecases were used both for the industrial and airport demand.

For IDM participation, after updates to prices and output forecasts of ND-RES, the VPP manager (or owner of each asset in case of No Coordination) makes adjustments to DAM auctions and in most cases, prioritizes the ND-RES over the D-RES units. Additionally, most updates are made in the earlier IDM sessions as evidenced in Fig 7 where there are no changes in offers made in IDM5 - IDM7.

### 2) Traded Power and Output of Assets on a Cloudy Day:

The VPP behaves differently on a day with intermittent cloud covers in the afternoon. There are more activities during IDM as the forecasts of ND-RES are in flux as shown in Fig. 3. This uncertainties, however, are taken care of by the model as observed in Fig. 9 (b) and Fig. 9 (c) where IDM bids reflect their expected behavior. With respect to demand, the early peak profiles were selected for both industrial and residential demands whereas the base case was retained airport demand.

The comparative advantage of the VPP over base case was the operation of the STU at the early hours. The STU charged the thermal storage instead of delivering energy from solar field to PB at lower efficiency, and thereafter delivered it at high PB efficiency while also capturing the high prices towards the end of the day as shown in Fig. 10 (b) and Fig. 10 (c).

### 3) Effects of Non-zero Cost on Demand Profile Choice:

Here, we provide a solution to the incentive structure for

demand owners. The default load profile has zero cost because the demand owner follows it irrespective of other events. The VPP then decides what price to pay the demand owners for other profiles such that the VPP's benefits are not eroded.

In Table I, the optimal choices of demand profiles are shown. Industrial and residential loads have the early peak and late peak as optimal profiles respectively. However, VPP manager is only willing to pay up to €320/day to the industrial load owner after which it is no more profitable for the VPP operation. In both of these demand cases, the industrial late peak profile is not profitable at all for the VPP and neither is the residential early peak profile. In the case of the airport demand, the early peak profile is profitable for the VPP manager as a cost up until €500/day while the late peak profile is only profitable until €305/day.

TABLE I  
DEMAND PROFILE CHOICE AT NON-ZERO COSTS

Demand	Basecase	Early peak	Late peak
Industrial	chosen when cost > €320/day	optimal	✗
Residential	chosen when cost > €180/day	✗	optimal
Airport	chosen when cost > €500/day	optimal	suboptimal - chosen when cost > €305/day

## V. CONCLUSION

This paper presents a heterogeneous RES-based VPP that participates in energy markets. Coupled with standard models of dispatchable resources, improved formulations of flexible demand and concentrated solar thermal plant were introduced to describe the technical operation of the VPP units. A network constrained unit commitment model is thereafter utilized by the VPP to participate in market activities. The energy market chosen in our study is the Spanish market.

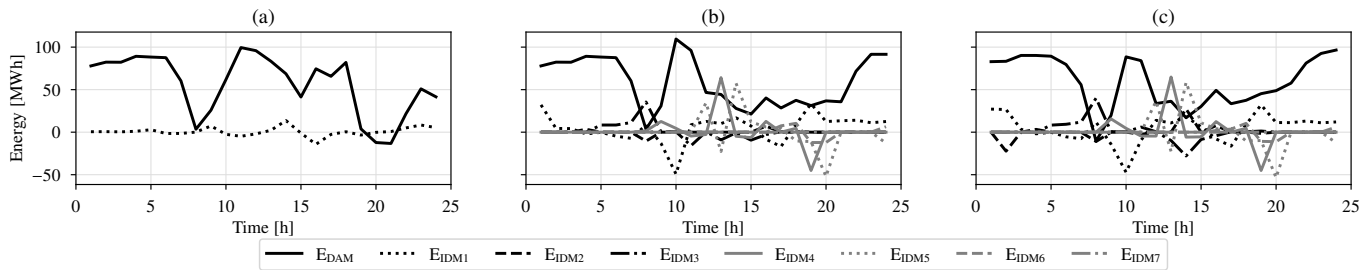


Fig. 9. Traded power on a cloudy day at DAM & IDM: (a) No Coordination, (b) VPP with default load profile, (c) VPP with three load profiles at zero cost

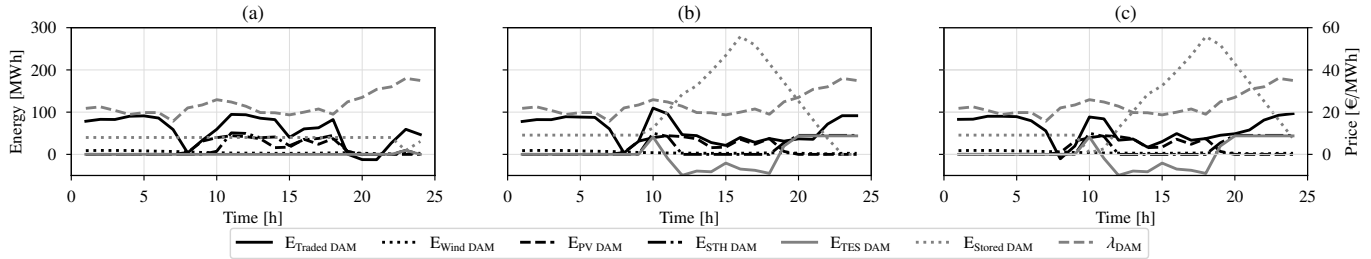


Fig. 10. Output of assets at DAM on a cloudy day: (a) No Coordination, (b) VPP with default load profile, (c) VPP with three load profiles at zero cost

Different case studies were then analysed to test the model's robustness against uncertainties due to weather conditions.

- 1) The VPP outperforms the case where the units are not coordinated by up to 20% on cloudy days.
- 2) VPPs incorporating flexible demand profiles with zero costs are the most beneficial compared to other configurations because the model selects the best profile that maximizes its profit.
- 3) When cost of demand profiles are non-zero, there are some thresholds which the VPP is willing to pay the demand owners until it becomes less profitable and they return to the default profile.
- 4) The impact of the STU with its storage was shown where the storage was charged at early periods while later discharging at higher capacity with higher efficiency. This led to higher profits of VPP over No Coordination in all conditions and especially during the cloudy days.

Future directions for this work include co-optimizing the DAM planning with secondary reserve market bids. This could ensure that there is available tolerance during real time operation. Application of the model to larger systems and considering AC power flow constraints will also be studied.

#### ACKNOWLEDGEMENTS

The authors wish to thank Mr. Ione Lopez with Iberdrola, Spain, and the people with CIEMAT, Spain, especially Dr Mario Biencinto and Dr. Loreto Valenzuela, that participated in the EU project POSYTYF, for the discussions on the modeling of solar thermal plants and flexible demands, and the provision of data used in the case study.

#### REFERENCES

[1] P. Pinson, L. Mitridati, C. Ordoudis, and J. Østergaard, "Towards fully renewable energy systems: Experience and trends in Denmark," *CSEE journal of power and energy systems*, vol. 3, no. 1, pp. 26–35, 2017.

[2] D. Koraki and K. Strunz, "Wind and solar power integration in electricity markets and distribution networks through service-centric VPPs," *IEEE Trans on Power Systems*, vol. 33, no. 1, pp. 473–485, 2017.

[3] R. Domínguez, A. Conejo, and M. Carrión, "Operation of a fully renewable electric energy system with CSP plants," *Applied energy*, vol. 119, pp. 417–430, 2014.

[4] R. Sioshansi and P. Denholm, "The value of concentrating solar power and thermal energy storage," *IEEE Trans on Sus Energy*, vol. 1, no. 3, pp. 173–183, 2010.

[5] G. He, Q. Chen, C. Kang, and Q. Xia, "Optimal offering strategy for CSPs in joint energy, reserve and regulation markets," *IEEE Trans on Sus Energy*, vol. 7, no. 3, pp. 1245–1254, 2016.

[6] S. Rohani, T. Fluri, F. Dinter, and P. Nitz, "Modelling and simulation of parabolic trough plants based on real operating data," *Solar Energy*, vol. 158, pp. 845–860, 2017.

[7] Z. Liu, W. Zheng, F. Qi, L. Wang, B. Zou, F. Wen, and Y. Xue, "Optimal dispatch of a virtual power plant considering demand response and carbon trading," *Energies*, vol. 11, no. 6, p. 1488, 2018.

[8] A. De La Nieta et al, "Local economic dispatch with local renewable generation and flexible load management," in *2018 SEST Conference*. IEEE, 2018, pp. 1–6.

[9] K. Herter, "Residential implementation of critical-peak pricing of electricity," *Energy policy*, vol. 35, no. 4, pp. 2121–2130, 2007.

[10] Z. Hungerford, A. Bruce, and I. MacGill, "The value of flexible load in power systems with high renewable energy penetration," *Energy*, vol. 188, p. 115960, 2019.

[11] A. Ciarreta, C. Gutiérrez-Hita, and S. Nasirov, "Renewable energy sources in the Spanish electricity market: Instruments and effects," *Ren. and Sus. Energy Reviews*, vol. 15, no. 5, pp. 2510–2519, 2011.

[12] "Operador del mercado ibérico de energía," <https://www.omie.es/en/>.

[13] "Red eléctrica de españa (REE)," <https://www.ree.es/en/>.

[14] J. P. Chaves-Ávila and C. Fernandes, "The Spanish intraday market design: A successful solution to balance renewable generation?" *Renewable Energy*, vol. 74, pp. 422–432, 2015.

[15] L. Baringo and M. Rahimiyan, "Virtual power plants and electricity markets," in *e-Book*. Springer, 2020.

[16] A Kargarian et al, "Toward distributed/decentralized DC optimal power flow implementation in future electric power systems," *IEEE Trans on SG*, vol. 9, no. 4, pp. 2574–2594, 2016.

[17] K. Van den Bergh, E. Delarue, and W. D'Haeseleer, "DC power flow in unit commitment models," *Energy and Environment*, vol. 240, 2014.

[18] I. L. García, J. L. Álvarez, and D. Blanco, "Performance model for parabolic trough STU with thermal storage: Comparison to operating plant data," *Solar Energy*, vol. 85, no. 10, pp. 2443–2460, 2011.

[19] B. AIMMS, "Aimms modeling guide—integer programming tricks," *Haarlem, The Netherlands: AIMMS BV*, 2018.